sustainability

MDPI

Article

Investigating the Impact of Various Vegetation Scenarios on Outdoor Thermal Comfort in Low-Density Residential Areas of Hot Arid Regions

Mohammed M. Gomaa [1,2,*], Adel El Menshawy [3], Jackline Nabil [4] and Ayman Ragab [2,*]

[1] Department of Architecture, School of Engineering, Computing& Design, Dar Al-Hekma University, Jeddah 22246, Saudi Arabia
[2] Department of Architectural Engineering, Faculty of Engineering, Aswan University, Aswan 81542, Egypt
[3] Architectural Engineering and Environmental Design Department, Arab Academy for Science, Technology and Maritime Transport, Alexandria 1029, Egypt; dradelsamy@yahoo.com
[4] Architectural Engineering and Environmental Design Department, Arab Academy for Science, Technology and Maritime Transport, Aswan 81511, Egypt; jackline_nabil@yahoo.com
* Correspondence: mgomaa@dah.edu.sa (M.M.G.); ayman.ragab@aswu.edu.eg (A.R.); Tel.: +966-564757907 (M.M.G.)

Abstract: In hot, arid regions, outdoor spaces suffer from intense heat. This study explores how vegetation can improve outdoor thermal performance for pedestrians in low-density residential areas. Specifically, it seeks to identify the best combination of grass and trees for optimal comfort. Four scenarios were simulated using ENVI-met software, varying the proportions of grass and three tree types: 50% grass, 50% grass with 25% trees, 50% grass with 50% trees, and 50% grass with 75% trees. A reference scenario with no vegetation was also investigated. The simulated outputs encompassed air temperature (Ta), mean radiant temperature (T_{mrt}), relative humidity (RH), and physiologically equivalent temperature (PET). The findings show that scenarios with a higher percentage of trees exhibited the best reduction in air temperature, ranging from 0.2 k to 0.92 k. Additionally, the inclusion of trees and grass in the scenarios resulted in a substantial improvement in thermal performance, with an average reduction of 7.5 degrees in PET. Among the evaluated scenarios, the one comprising 75% trees and 50% grass exhibits the most noteworthy enhancement. This study underscores the significance of strategically positioning vegetation to coincide with prevailing wind patterns, thereby enhancing convective cooling mechanisms and improving overall thermal comfort levels. These insights offer valuable implications for urban planning and the development of sustainable design strategies.

Keywords: green adaptation; urban microclimate; ENVI-met; Outdoor Thermal Comfort (OTC); heat mitigation; physiologically equivalent temperature (PET)

Citation: Gomaa, M.M.; El Menshawy, A.; Nabil, J.; Ragab, A. Investigating the Impact of Various Vegetation Scenarios on Outdoor Thermal Comfort in Low-Density Residential Areas of Hot Arid Regions. *Sustainability* **2024**, *16*, 3995. https://doi.org/10.3390/su16103995

Academic Editors: Siu-Kit Lau, Vesna Kosoric, Abel Tablada, Miljana Horvat, Milena Vukmirović, Silvia Domingo-Irigoyen, Marija Todorović, Jérôme H. Kaempf, Kosa Golić, Ana Peric and Tatjana Kosić

Received: 26 March 2024
Revised: 26 April 2024
Accepted: 6 May 2024
Published: 10 May 2024

1. Introduction

Global warming-induced temperature increases across diverse regions are projected to substantially impact outdoor and indoor thermal comfort, posing significant threats to human health in the coming decades [1]. The effectiveness of climate has attracted the attention of many urban planners due to the documented increase in atmospheric temperatures in urban regions, particularly in hot, arid climatic zones [2]. The temperature rise could be attributed to the manifestation of the Urban Heat Island (UHI) phenomenon, which impacts numerous urban areas. The UHI phenomenon is distinguished by a pronounced elevation in air temperature within urban regions compared to the adjacent rural areas. As cities expand, urban sprawl increases heat trapped by human activities, heat-absorbing surfaces like asphalt, air pollution, and the loss of green spaces [3].

In metropolitan regions, pedestrian-induced urban heat islands (UHIs) significantly influence human well-being and thermal satisfaction. The absence of green spaces primarily contributes to thermal discomfort in urban outdoor environments. Numerous studies have indicated that urban areas in warm climatic conditions tend to use limited spaces by substituting heat-absorbing land surfaces with natural cover [4–6]. This phenomenon occurred because of the substitution of indigenous plants with surfaces that possess the capacity to assimilate solar radiation and retain heat. The phenomenon can be attributed to the materials' thermal and optical characteristics. Specifically, artificial substances like asphalt pavements and concrete edifices can absorb and retain solar radiation. Unlike their natural surroundings, they exhibit notable moisture resistance, reducing the likelihood of evaporative cooling. Recently, more emphasis has been placed on understanding the relationship between urban features and local climate and devising mitigation and adaptation techniques to enhance urban thermal performance [7,8]. Several studies on the effects of various urban geometrical thermal mitigation measures on outdoor spaces have been conducted for hot, arid climate zones [9–12].

The geometrical variables of urban environments explored in the evaluated studies are divided into two categories (squares and plazas, canyons) [13–16]. The canyon-like shape of buildings and streets also traps heat in metropolitan regions. Squares and plazas have geometrical variables such as the aspect ratio and sky view factor (SVF). These variables are determined by the characteristics of those spaces, which are associated with the urban pattern's shape and geometry [17]. The prevailing meteorological conditions directly influence outdoor thermal comfort, a state of mind expressing satisfaction with the ambient thermal environment [5,18]. Several studies have employed the physiologically equivalent temperature (PET) index [19–21]. The PET index combines the influences of air temperature, humidity, wind speed, and radiation fluxes into a single representative value. As an empirical heat-balance model calibrated to a physiological response, PET provides an updated assessment of individuals' outdoor thermal conditions.

Evaluating outdoor thermal comfort is based on the concept of human energy balance. This concept recognizes the human body's capacity to thermoregulate and adapt to different microclimates. As depicted in Figure 1, the study emphasizes the significance of the physiological equivalent temperature (PET) and its relation to thermal perception [22]. PET serves as a valuable tool for evaluating the thermal characteristics of diverse climates [23]. Furthermore, it is widely recognized as an outdoor thermal comfort indicator, investigating the influence of urban geometric attributes on thermal conditions across various weather conditions [24,25]. The PET index incorporates multiple environmental factors, including air temperature, relative humidity, wind speed, and solar radiation, to provide a comprehensive assessment of the outdoor thermal conditions.

Cities striving to enhance urban thermal environmental performance employ various mitigation strategies to improve thermal conditions within urban areas. Design techniques incorporating urban geometry considerations, such as sky view factor (SVF), aspect ratio, and shading scenarios, play a significant role in these efforts. Several well-established strategies are employed to mitigate urban heat island effects, including solar-reflective cool roofs, solar-reflective cool pavements, vegetative green roofs [26], and increased street-level urban vegetation [5,27,28]. Furthermore, different vegetation scenarios can substantially influence the cooling impact in outdoor urban spaces. Urban vegetation provides shade for buildings and surfaces, leading to lower urban temperatures through two mechanisms: enhanced evaporative heat flux and reduced sensible heating. The cooling effect is more pronounced with higher canopy density, improving human thermal comfort [29]. These strategies effectively address the challenges of urban heat mitigation and contribute to creating more thermally comfortable urban environments.

PET (°C)	Thermal Perception	Grade of Physiological Stress
<4	Very cold	Extreme cold stress
4–8	Cold	Strong cold stress
8–13	Cool	Moderate cold stress
13–18	Slightly cool	Slight cold stress
18–23	Comfortable	No thermal stress
23–29	Slightly warm	Slight heat stress
29–35	Warm	Moderate heat stress
35–41	Hot	Strong heat stress
>41	Very hot	Extreme heat stress

Figure 1. The relationship between the PET index, the perceived thermal sensation, and physiological heat stress experienced by humans.

In this research, we seek to quantify the optimal percentage of vegetation that can contribute to thermal comfort in hot, arid climates, especially in low-density built-up residential districts, by integrating multiple elements of vegetation, including trees and grasses. ENVI-met has been used as a simulation tool, which predicts the consequences of large structural changes like alternative building constellations and the interactions between small structural changes and local climate resulting from the urban pattern form and geometry [30]. This study has important implications for urban planners and policymakers seeking to advance sustainable development and mitigate the adverse effects of climate change and urban heat island effects.

2. Literature Review

Numerous studies have extensively assessed the influence of vegetation and land covers on the thermal performance of urban environments [31–35]. One of these studies investigated the effectiveness of trees in mitigating the UHI effect and reducing energy consumption in built-up areas of Cairo [36]. The findings of this research emphasized that the density of the built-up area influences the trees' cooling effect. In high-density areas, trees demonstrated a notable cooling impact, decreasing the daily air temperature by approximately 0.2–0.4 k. However, the trees had the opposite effect in low-density areas, increasing air temperatures of up to 3.0 k. This disparity can be attributed to the interplay of humidity and evaporation processes. These findings underscore the significance of considering the urban context and density when implementing vegetation-based strategies to mitigate the UHI effect and enhance outdoor thermal comfort effectively.

Another investigation explored the impact of modifying land cover on surface and air templates within micro-scale localized urban areas. Their findings revealed a distinct temperature distribution, with asphalt exhibiting the highest temperatures, followed by soil, grass, water, and forest. However, as the number of measurement points increased, the spatial pattern of hot and cool spots became more evident at the surface level. The temperature contrast between hot and cool spots decreased with increasing height, showing a difference of 4.1 °C at 0.1 m and 3.1 °C at 1.5 m [3].

Srivanit and Hokao conducted a separate study that investigated the impact of tree density and rooftop grass layers on air temperature reduction, particularly during the peak of summer. Increasing the tree density by 20% leads to an average maximum temperature decrease of 2.27 °C during the summer peak at 15:00. Combining both greening strategies, i.e., combining trees to existing green areas and introducing rooftop grass layers on educational buildings, yielded the most significant air temperature reduction, with a temperature decrease between 0.24 °C to 2.29 °C [37]. Another study by Jim found that

vegetated roofs exhibited lower maximum and minimum temperatures during the day compared to non-vegetated roofs [34].

Taleghani et al. examined the influence of street trees, cool pavements, and green roofs on air temperature and thermal comfort in urban environments [5]. Their findings indicated that incorporating more street trees and cool pavements significantly reduced air temperature by 1.5 k. However, these benefits were primarily confined to the pedestrian level. Conversely, cool and green roofs offered cooling effects higher above but had minimal impact on ground-level comfort. Interestingly, cool pavements were observed to increase reflected sunlight reaching unshaded pedestrians, potentially reducing their thermal comfort.

In areas with existing tree cover and adjacent to roadways, implementing cool pavements significantly decreased the surface air temperatures during the day, with minimal changes in mean radiant temperature. Consequently, this resulted in a decrease in PET of 1.1 °C, thereby improving thermal comfort. Contrarywise, adding street trees proved to be the most effective strategy for enhancing the outdoor thermal comfort of pedestrians in unshaded sites during the afternoon. In contrast, cool pavements demonstrated the most substantial improvements in afternoon thermal comfort in shaded sites near streets. Green and cool roofs exhibited the lowest effect on pedestrian thermal comfort as they primarily influenced the energy balance at the roof level, which is well above the height of pedestrians [5].

A comprehensive investigation examined how the built geometry and morphology impact the outdoor thermal environment within a university campus situated in a hot and humid urban area [38]. The research encompassed two main aspects. Firstly, field measurements were employed to assess the impact of built geometry on microclimatic conditions. Secondly, a survey was conducted to evaluate the students' perceptions of the outdoor thermal environment in a hot and humid climate. The findings of this study revealed that various built parameters, including the sky view factor (SVF), building materials, and green cover, significantly influenced microclimatic conditions and daytime thermal sensation. Specifically, the presence of vegetation and its shading effect played a crucial role in reducing air temperatures and PET values during the day, irrespective of location orientation. Furthermore, internal shading of buildings was found to contribute to increased pedestrian comfort [39]. This highlights the effectiveness of vegetation in mitigating the UHI effect and enhancing outdoor thermal comfort.

Fahmy and Sharples conducted a study focusing on the passive thermal comfort potential of a parallel and linear clustered form of urban trees in Cairo, Egypt [31]. Despite the high temperatures indicated by the predicted mean vote (PMV) values, reductions in PMV values were observed within the cluster courtyards, even with low closure ratios that would typically lead to more significant reductions. It should be noted that these results were influenced by the simulation of a critical day under Cairo's hot, arid conditions and potential software overestimations [40].

Investigating the impact of vegetation cover and urban density on the urban heat island effect, the findings by Chapman et al. showed that vegetation exhibited greater effectiveness in reducing nighttime temperatures compared to daytime temperatures [33]. On the other hand, Weng et al. conducted a study examining the relationships between land surface temperatures (LST), impervious surface fraction, and green vegetation fraction in Indianapolis, United States. The research revealed a positive correlation between LST and impervious surface fraction, while a negative correlation was observed between LST and green vegetation fraction. The study also identified specific relationships between LST and urban morphology, with each temperature zone associated with a dominant land use and land cover (LULC) category [35].

Examining the impact of vegetation on external thermal comfort in hot, arid regions, focusing on the Algerian Sahara as a case study, Dohssi et al. analyzed various environmental factors such as air temperature, humidity, radiation, and surface temperature. Thermal comfort indices were also considered, including predicted mean vote (PMV) and PET.

Their findings emphasized the significant role played by vegetation in enhancing thermal comfort within urban environments situated in hot, arid climates. The presence of plants and trees was found to moderate microclimate conditions, leading to improved thermal sensations and physiological responses for individuals in outdoor spaces [41].

Louafi et al. investigated the influence of vegetation cover on thermal and visual comfort in hot, dry urban environments. Their analysis of microclimate variables and comfort indices revealed that dense vegetation significantly optimized conditions and enhanced pedestrian thermal and visual comfort in challenging settings. Greenery was found to reduce air temperatures, increase humidity, and provide shading, improving overall outdoor comfort experiences [42].

3. Case Study

Aswan is located in the southern region of Egypt (Figure 2), characterized by a hot, arid climate and extreme temperature variations. During summer, daytime temperatures in Aswan City can exceed 45 °C, while in winter, they can drop below 15 °C. The relative humidity in this region follows distinct seasonal patterns. The lowest relative humidity values, around 12%, are typically observed in July and August. Conversely, the highest relative humidity values, reaching 36% and 34%, are recorded in December and January, respectively [43]. EL-Khazzan residential district in Aswan was selected as the research site based on its suitability for the study. Figure 3 depicts the location of EL-Khazzan in the far south of Aswan, approximately 9 km from the airport.

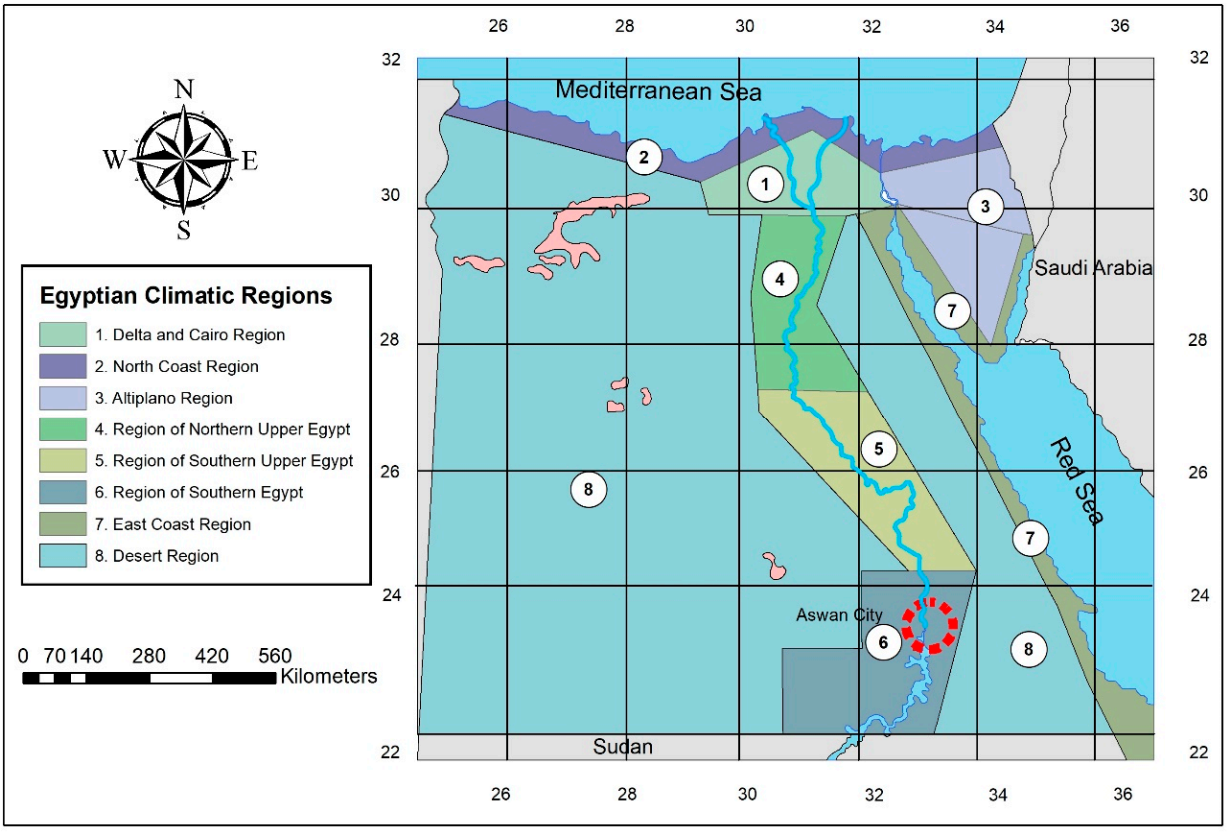

Figure 2. Egyptian climatic region showing the location of Aswan City.

This region is characterized by a hot and dry desert climate, which makes it an ideal candidate for investigating the influences of vegetation types on thermal comfort in such environments. The total area of the residential district encompasses 33,800 m^2, with 13% of the area being built up, as indicated by the land use ratio presented in Table 1. The district consists of one-story residential buildings constructed with a structural system comprising

bearing walls. Each residential block has a standard area of 130 m^2. Figure 4 illustrates that the aspect ratio of the district is 1/2, including streets that are 10 m wide and a height of 5 m for buildings. Notably, each residential block is accompanied by a green yard, which adds to the overall vegetation cover in the area. Despite being a low-density built-up area, EL-Khazzan serves as a valuable case study for investigating the influence of different vegetation types on outdoor thermal comfort in low-density areas.

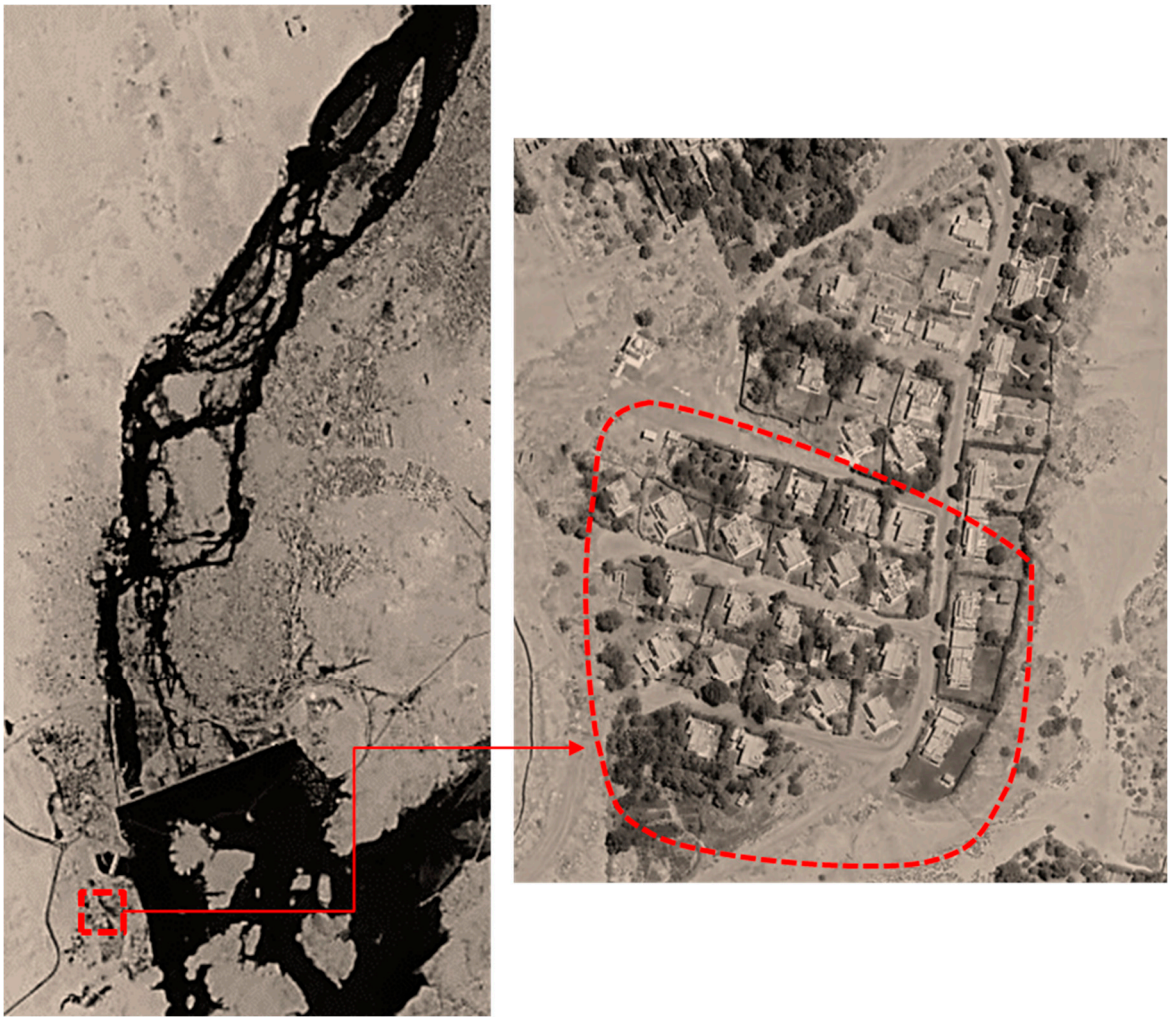

(**a**) (**b**)

Figure 3. (**a**) Aerial view of Aswan City showing the location of the studied area; (**b**) Detailed map showing El-Khazan residential district.

Table 1. Land use ratio for EL-Khazzan case study.

Usage	Area	Percentage (%)
Built up area	4420	13
Streets and pedestrian area	29,380	87
Total areas	33,800	100

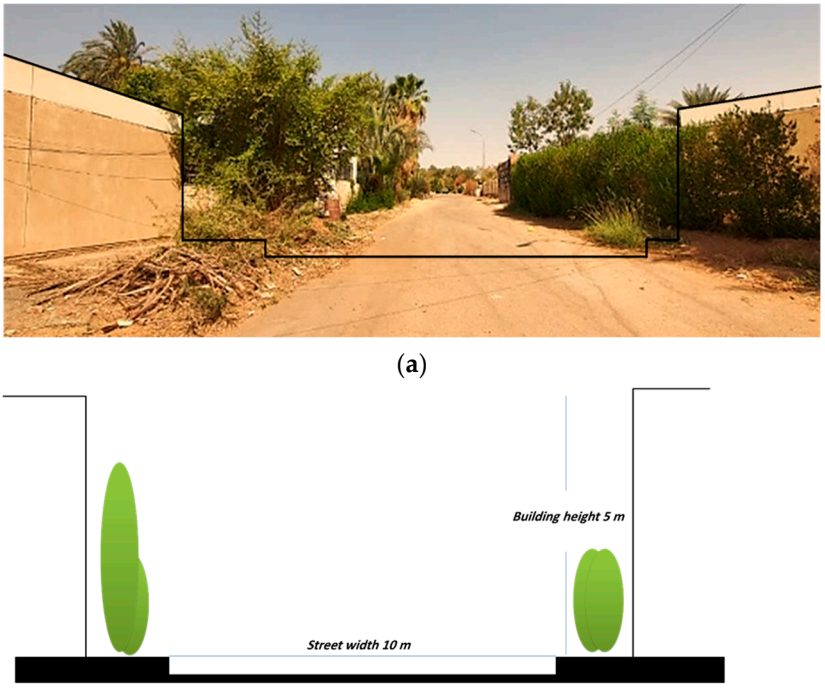

Figure 4. Aspect ratio for street in the studied residential area, (**a**) street model; (**b**) conceptual section showing the street width and building height.

4. Methodology

This study used a coupling method to comprehensively evaluate the effectiveness of various greening scenarios on the thermal performance of a residential district microclimate. Figure 5 presents the main phases to achieve the study aim: (1) The on-site measurements were conducted to capture the current microclimate conditions at the pedestrian level in the residential district. The collected data were obtained to gain insights into microclimate thermal performance. Recently, it was used to validate the simulated study model. (2) ENVI-met 5.5.1 software simulated the current case and other proposed mitigation scenarios. These scenarios included the addition of trees, grass, and a combination of both.

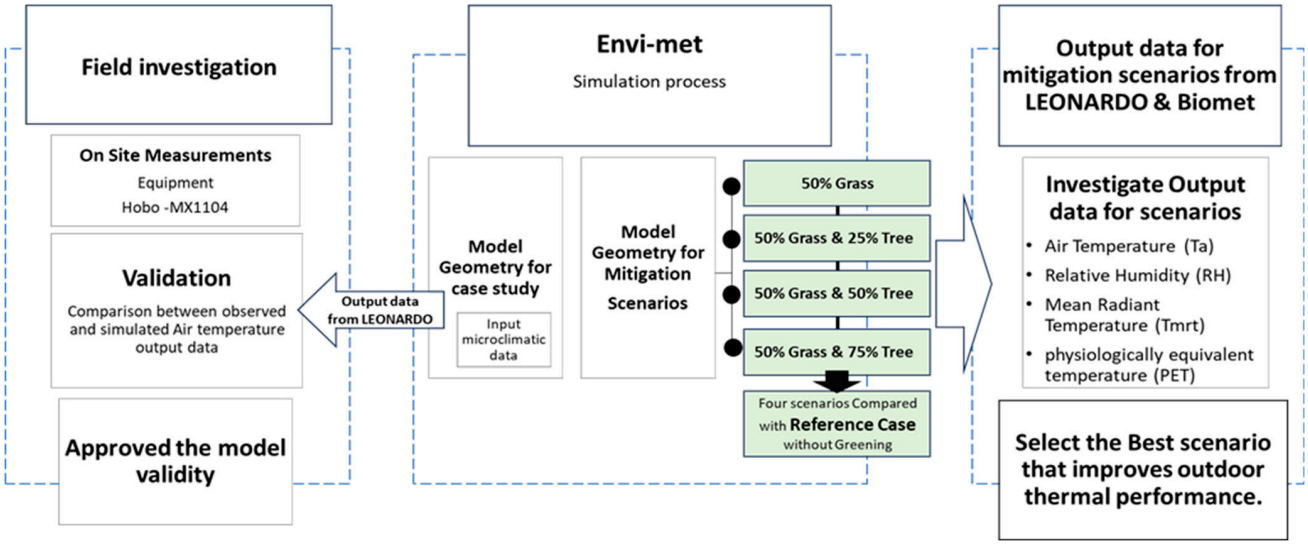

Figure 5. Flowchart for the overall research design.

4.1. ENVI-Met Microclimate Model

The ENVI-met version 5.1.1 software was utilized to simulate a microscale environment for the case study. The input parameters employed in the ENVI-met modeling process are presented in Table 2. This study employed full-forcing weather data boundaries obtained from the Aswan University weather station for the investigated date. It implements a 24-h forcing of air temperature (Ta) and relative humidity (RH). The provided maximum and minimum Ta values were 44.4 °C and 30.17 °C, respectively, while the maximum and minimum RH values were 34.4% and 15.7%, respectively. The grid dimension for the simulation was set at 100 m × 100 m, allowing for a detailed analysis of the study area. The core domain size was defined as 300 m × 300 m, and the vertical and horizontal grid sizes are 3 m, which indicates that the simulation can capture fine-scale variations in temperature. The fact that the highest building in the domain is 5 m suggests that the simulation is focused on a relatively flat urban area with low-rise buildings.

Table 2. Input parameters for ENVI-met modeling.

Parameter	Value
Grid dimension	100 × 100 × 30 Grids dx = 3.00 m, dy = 3.00 m, Base dz = 3.00 m.
Core XY domain size	x = 300, y = 300
Soil profile for all grids	Sandy soil for the neighborhood boundary, Loamy soil and pavement around the buildings, and asphalt for streets.
Floor albedo	Albedo values as follows: sandy soil 0.31, loamy soil 0.1, pavement 0.5, asphalt 0.12
Material emissivity	Emissivity values as follows: sandy soil 0.85, loamy soil 0.9, pavement 0.92, asphalt 0.95
Thickness of wall materials (m)	0.02 Cement plaster, 0.25 Brick wall, and 0.02 Cement plaster
Façade albedo	0.2
Roof materials	Reinforced concretes thickness = 0.3 m.
Simulation date	24 h on 13 August
Metabolic rate for persons (met)	1.48
Clothes (clo)	0.9
Start wind speed (m/s)	2
Start wind direction	315°
Initial specific humidity of atmosphere (g/kg)	8

4.2. Field Investigation and Model Validation

To validate the accuracy of the ENVI-met model, the simulated air temperature and relative humidity values were compared to real data collected on-site through monitoring equipment. On-site measurement data were collected in the EL-Khazzan study area at a specific location designated as a reference point (P). For the measurements, Onset-Hobo-MX1104 data loggers (Onset Computer Corporation, Bourne, MA, USA) were installed at a height of 1.5 m, as depicted in Figure 6. It demonstrates high accuracy in measuring temperature (−20 °C to 70 °C), relative humidity (0% to 100%), and light intensity (0 lux to 167,731 lux) [44]. The measurements were taken continuously for 24 h on 13 August, characterized by hot and sunny weather conditions. The 13th of August was chosen as it reflects the general weather patterns and conditions commonly experienced during the summer season in the city. Using data loggers was instrumental in ensuring precise and dependable measurements of microclimate variables. The simulation was created using the ENVI-met 5.1.1 software to model the current situation. Real local data for 13 August

2023, obtained from the Aswan University weather station, were entered into the ENVI-met software as input data to generate the simulation.

(**a**) (**b**)

Figure 6. (**a**) On-site measurement at a specific point (P), (**b**) Onset-Hobo -MX1104 device.

Figure 7a,b illustrates the comparison between simulated and observed air temperatures and relative humidity, revealing a notable similarity pattern. The variation between simulated and observed air temperatures ranged from 1.2 to 3.2 °C, indicating a successful alignment between the simulated and monitored models in terms of air temperature. Similarly, the variation between simulated and observed relative humidity ranged from 0.04 to 4.24%. The strong correlation observed between ENVI-met and monitored climatic data further supports the model's accuracy in representing and simulating air temperature and relative humidity variations.

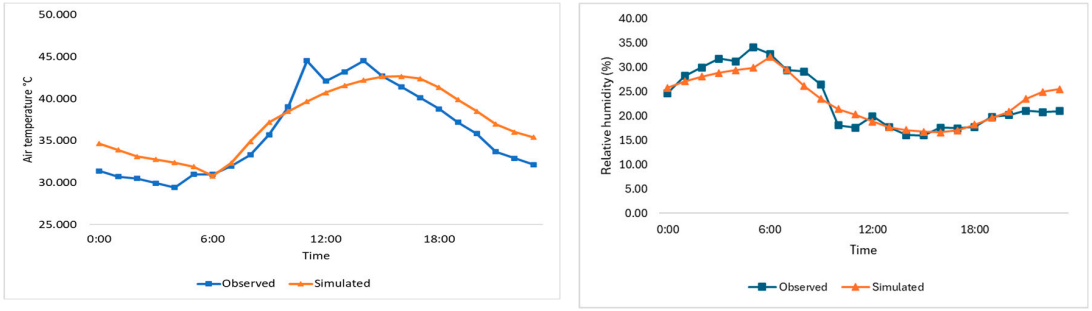

(**a**) (**b**)

Figure 7. Comparison between observed and simulated (**a**) Air temperature and (**b**) relative humidity for point "P" at 1.5 m.

To ensure the reliability and accuracy of the ENVI-met model, a thorough validation process was conducted using the root mean square error (RMSE) metric. The RMSE values for air temperature and relative humidity were 2.44% and 2.24%, respectively, falling within the tolerance criteria set by the American Society of Heating, Refrigerating, and Air-Conditioning Engineers (ASHRAE) with a ±20% threshold for RMSE [45,46]. Additionally, the coefficient of correlation (R2) recorded at 0.84 and 0.86 for air temperature and relative humidity, respectively, as depicted in Figure 8a,b, further corroborates the successful validation of the ENVI-met model regarding air temperature and relative humidity.

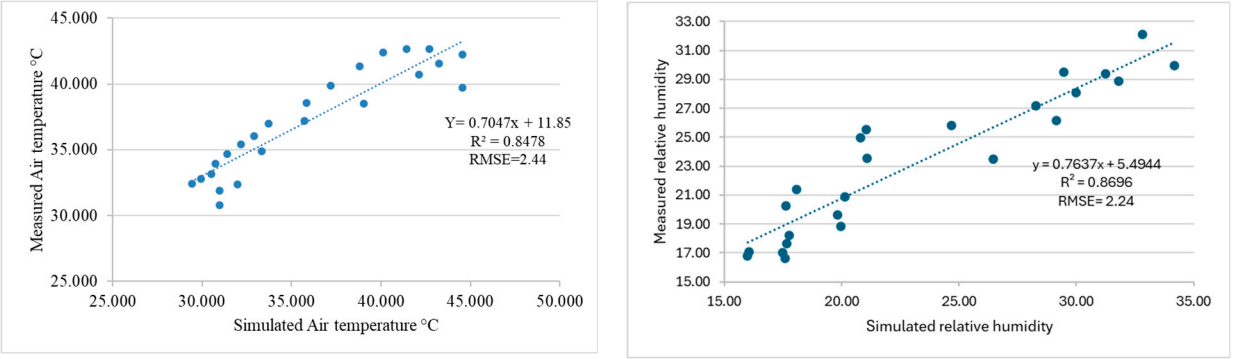

(**a**) (**b**)

Figure 8. Quantifying agreement between measured and simulated (**a**) air temperatures and (**b**) relative humidity on 13 August.

4.3. The Criteria to Design the Proposed Scenarios

Three distinct types of trees have been used in this study due to their previous efficacy in mitigating thermal heat within hot, arid regions, based on the study conducted by Fahmy et al. [47]. A new method was used to utilize the measurements of LAI, Albedo, and canopy geometrical parameters of three common Egyptian urban trees for numerical modeling. The results showed that trees with denser foliage and higher radiation reflectivity exhibited increased evapotranspiration, incident radiation reflection, absorption, and shading effects. Table 3 explains the specifications of these trees, including *Cassia leptophylla*, *Cassia nodosa*, and *Ficus nitida*.

Table 3. Specification of investigated trees.

Specification	**Name of Tree**		
	Cassia leptophylla	*Cassia nodosa*	*Ficus nitida*
			
Total tree height	12 m	5 m	3 m
Maximum LAD height	9 m	4 m	2 m
Foliage height	8 m	3 m	2 m
LAI	3.185	3.499	3.986
Albedo	0.085	0.085	0.09

It has been observed that the *Ficus nitida* species is most effective when applied to the boundary of the urban site. This is due to the species' ability to provide shading and reduce solar radiation exposure to the surrounding environment. *Ficus nitida* is not necessarily the smallest of the three-tree species mentioned. However, it is still effective when applied to the boundary of an urban site due to its ability to provide ventilation and shade on site. On the other hand, *Cassia leptophylla* and *Cassia nodosa* are most effective when applied in the

urban form core. The vegetation percentage is a crucial criterion for improving outdoor thermal comfort. In Figure 9, the criteria for the distribution of trees according to their type and specifications are illustrated. All the proposed scenarios were simulated and compared to the reference case output data to explore the most effective vegetation percentage for improving thermal comfort in the El Khazan residential district.

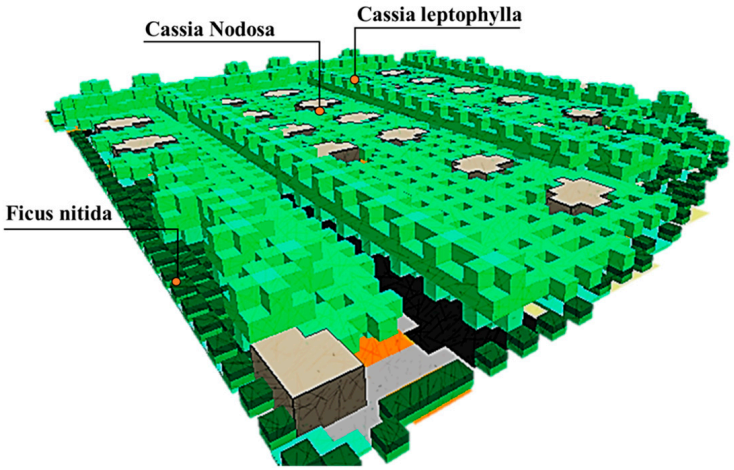

Figure 9. The distribution of the urban trees by their types for the scenario adding 50% grass and 75% trees.

In this regard, thermal performance was evaluated using key indicators such as air temperature (T), relative humidity (RH), and mean radiant temperature (T_{mrt}). The data were collected from four specific points within each simulated scenario, and the thermal condition was investigated throughout the district. Then, the extracted output data were compared to the reference case. Vegetation scenarios are designed to leverage the cooling and shading benefits of trees and the reflective properties of grasses to reduce heat buildup and improve thermal comfort. These scenarios could be divided into four different vegetation percentages, as shown in Table 4. Furthermore, the proposed scenarios were gradually designed to include 25% to 75% tree percentages, with the grass percentage assumed to be 50% of the total district outdoor area. In this regard, Sc-A exhibited 50% grass without trees. Sc-B is 50% grass and 25% trees. Sc-C is 50% grass with 50% trees. Finally, Sc-D is 50% grass and 75% trees.

Table 4. Design of reference case without greening and mitigation scenarios.

Name	Description		Two-Dimensional Site Plan for Simulated Scenarios	Three-Dimensional Site Plan for Simulated Scenarios
	Grass Percentage (%)	Trees Percentage (%)		
Reference scenario	0%	0%	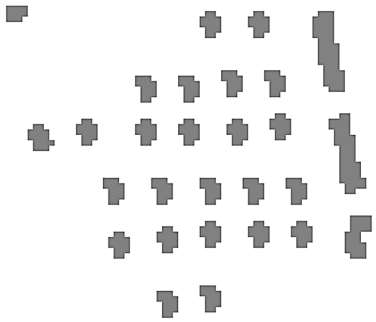	

Table 4. *Cont.*

Name	Description		Two-Dimensional Site Plan for Simulated Scenarios	Three-Dimensional Site Plan for Simulated Scenarios
	Grass Percentage (%)	Trees Percentage (%)		
Sc-A	50%	0%		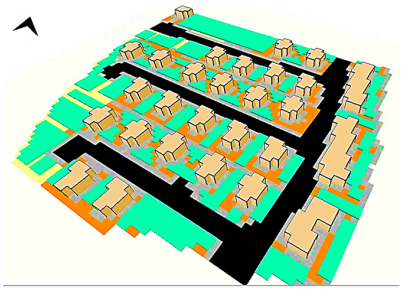
Sc-B	50%	25%	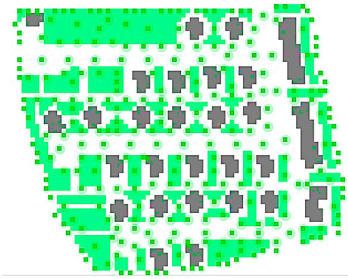	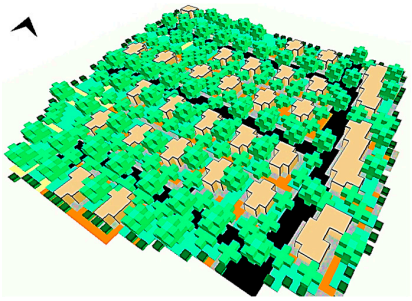
Sc-C	50%	50%	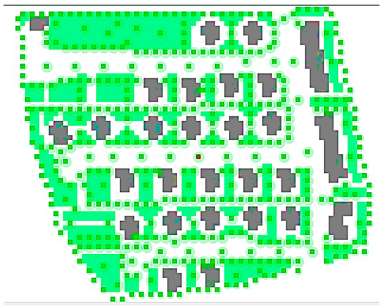	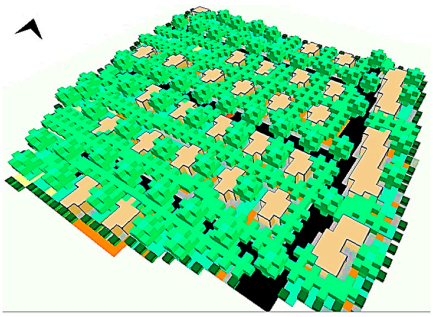
Sc-D	50%	75%		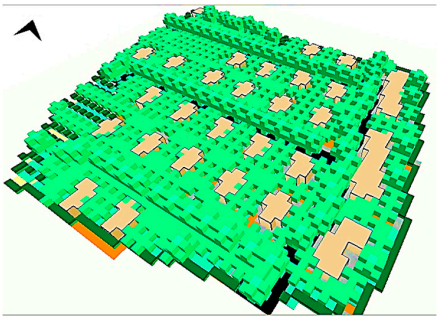

5. Results

This research illustrates the specific locations of the four points: R1, R2, R3, and R4. These points are situated in various locations and are exposed to varying degrees of shading and different materials for covering land at each location, as shown in Table 5. R1 is located adjacent to a residential block on pavement and is shaded by the adjacent building; R2 is situated on the street (with a land cover of asphalt material). Leptophylla trees also shade this point. R3 is also located in a setback area for a residential block but on pavement rather than grass-covered land. A *Cassia nodosa* tree also shades this point. R4 is located

on grass-covered land in the buffer zone, characterized by a wide free space without any obstructions. Leptophylla trees shade this point.

Table 5. Location and description of measurement points.

Two-Dimensional Site Plan	Side View
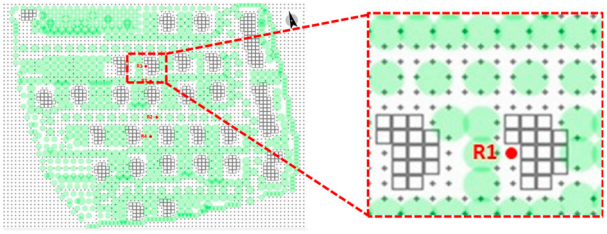	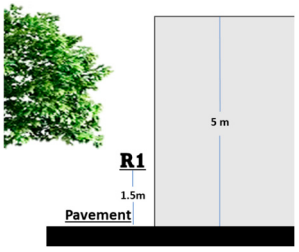
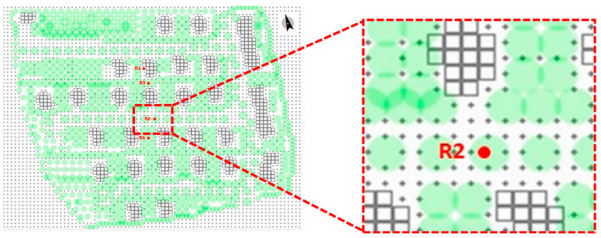	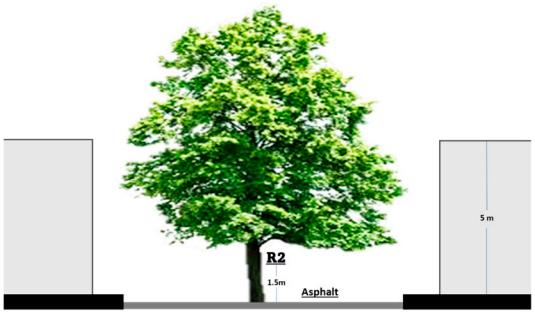
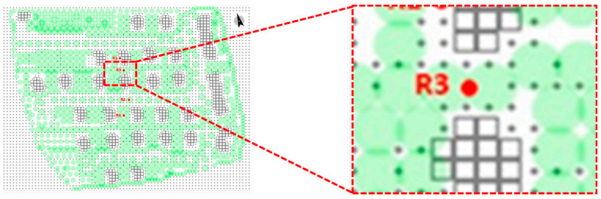	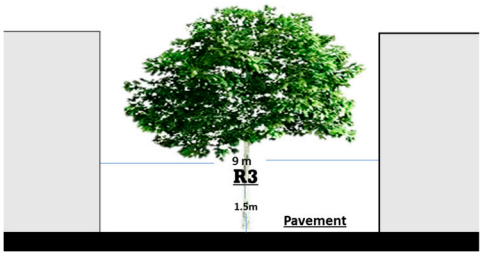
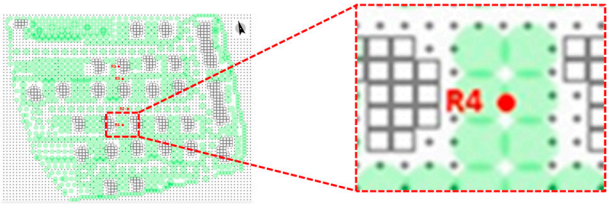	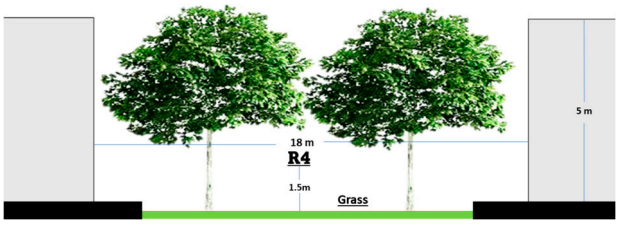

5.1. Air Temperature

The observed improvements in air temperature in all mitigation scenarios, particularly those involving trees, were relatively minimal. A consistent performance was observed across all measured points (R1, R2, R3, and R4). Figure 10 presents the temperature differences, expressed in degrees, between the vegetation and reference scenarios over 24 h.

The outcomes of four vegetation scenarios are compared with a reference scenario. From 8:00 a.m. to 7:00 p.m., Sc-A, which included the addition of 50% grass, resulted in a reduction ranging from 0.02 k to 0.275 k; in Sc-B, where 25% trees and 50% grass were added, a reduction ranging from 0.12 k to 0.67 k was recorded. Sc-C, which included 50% trees, reduced from 0.13 k to 0.78 k. Lastly, Sc-D with 75% trees exhibited the best reduction, ranging from 0.2 k to 0.92 k. On the other hand, from 8:00 p.m. to 05:00 a.m., during the night, Sc-A reduced air temperature by 0.2 k. However, at Sc-B, it should be noted that one measurement point, R1, located beside a building, exhibited an increase from 8:00 a.m. to 3:00 p.m., which increased by an average of 0.45 k. However, it exhibited a larger reduction

of 0.5 k compared to reference scenarios. This discrepancy can be attributed to the surface radiation and the moisture generated by the limited presence of trees in contrast to Sc-C and Sc-D, where the inclusion of 50% grass and 75% trees led to an air temperature increase during the night, ranging from 0.2 k to 0.6 k. The presence of trees can disrupt natural airflow patterns.

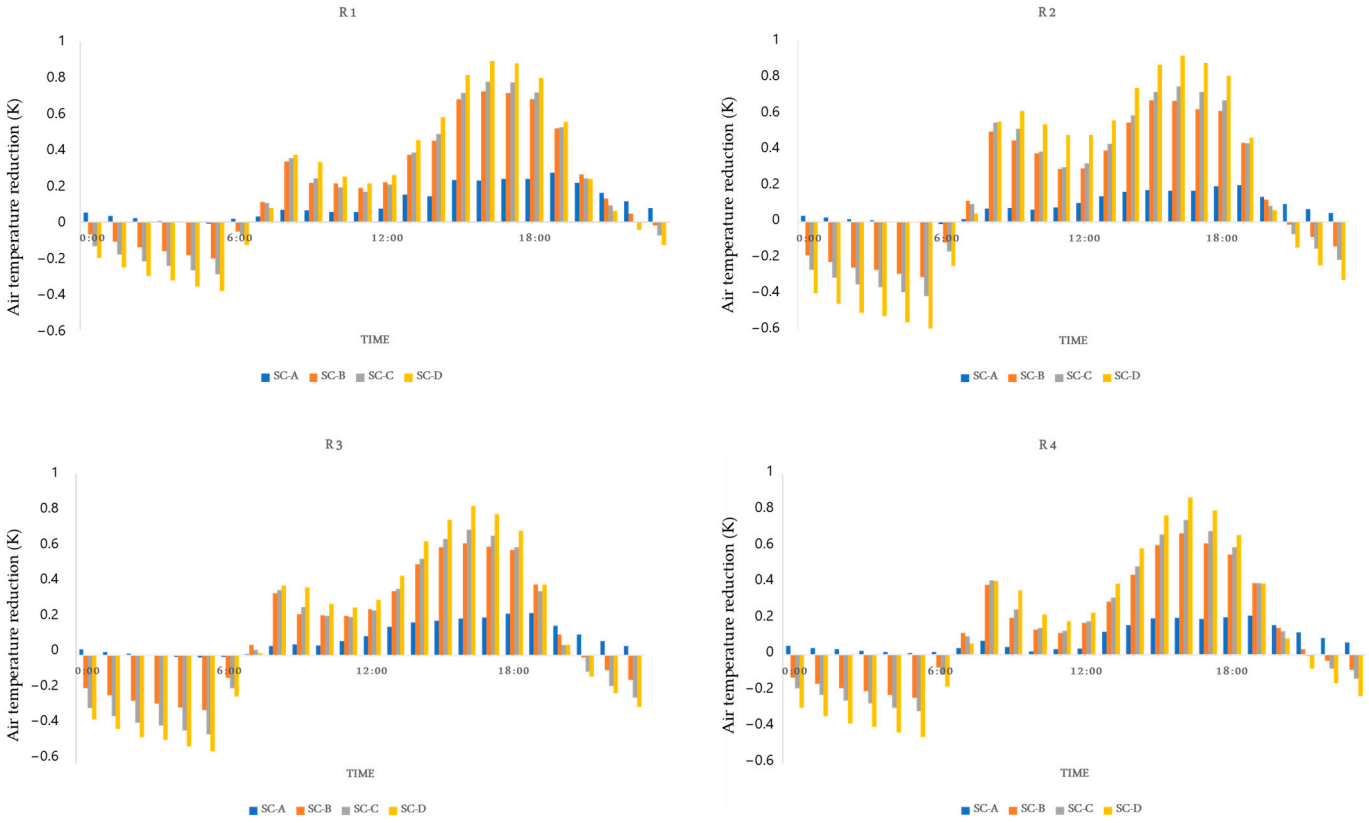

Figure 10. Air temperature (Ta) differences at R1, R2, R3, and R4 between the reference scenario and mitigation scenarios A, B, C, and D.

During the day, trees can create shade and induce evaporative cooling by transpiring water through their leaves, which can have a cooling effect. However, during the night, the disrupted airflow caused by the trees can impede air exchange between the immediate vicinity and the surrounding cooler air, leading to a stagnant air mass that can increase temperatures. While these reductions positively impact air temperature, they are relatively modest in magnitude.

5.2. Relative Humidity

The observed rise in relative humidity (RH) across all mitigation scenarios was relatively modest. Consistent performance was evident across all measured points (R1, R2, R3, and R4). Figure 11 illustrates the RH differences between the vegetation and reference scenarios over 24 h. Comparing the outcomes of four vegetation scenarios with a reference scenario, it is noted that from 7:00 a.m. to 7:00 p.m., Sc-A demonstrated an average RH increase ranging from 0.018% to 0.263%. Sc-B exhibited an RH increase ranging from 0.33% to 0.95% during daylight hours. Sc-C demonstrated an RH increase from 0.35% to 1.2%, while Sc-D exhibited the highest RH increase from 0.4% to 1.5%. During the night, specifically from 8:00 p.m. to 05:00 a.m., Sc-A witnessed a consistent 0.1% increase in RH across all measured points. Sc-C and Sc-D increased RH during nighttime hours, ranging from 0.1% to 0.7%.

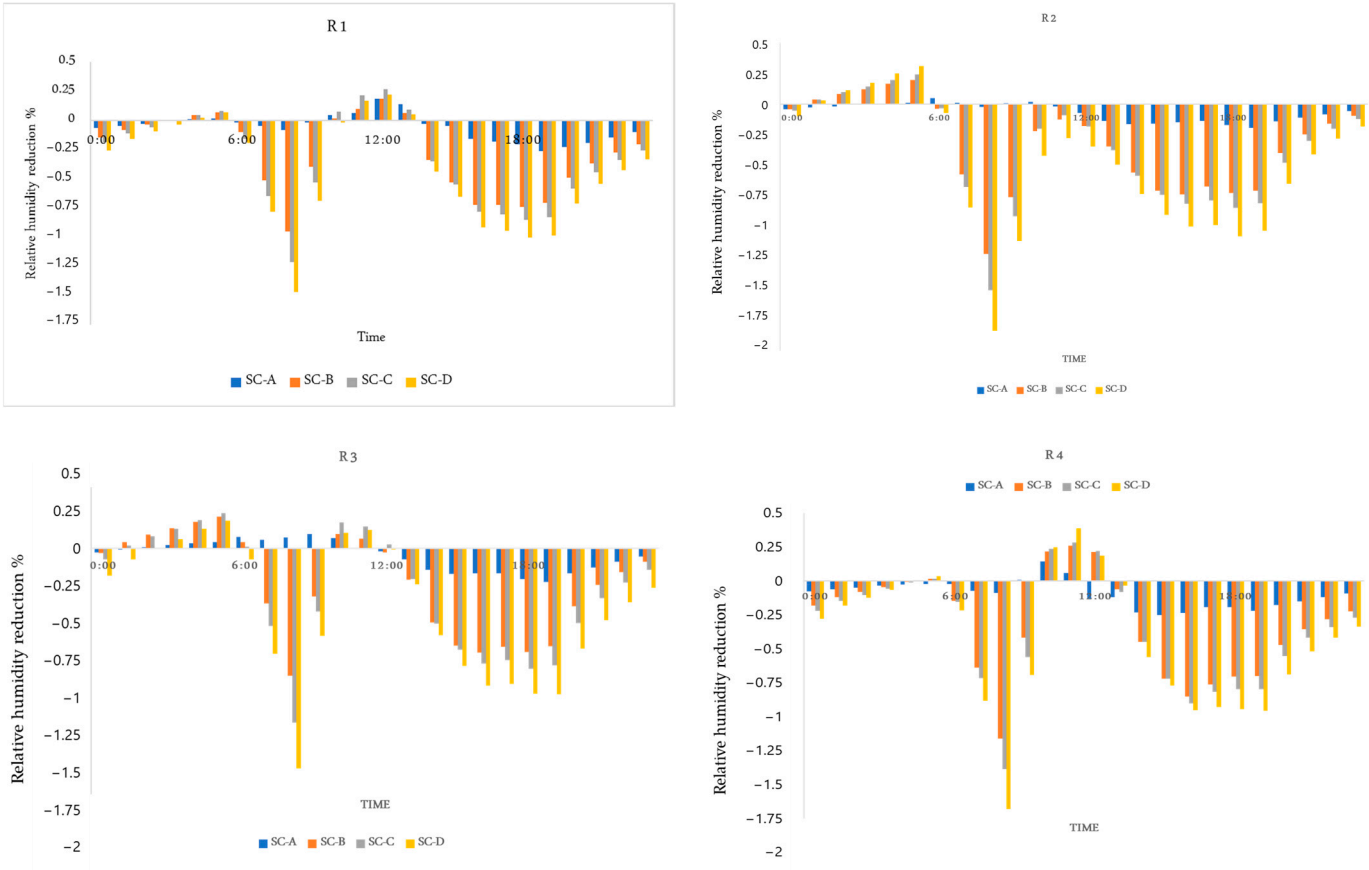

Figure 11. The differences in Relative humidity (RH) at R1, R2, R3, and R4 between Reference scenario and mitigation scenarios A, B, C, and D.

5.3. Mean Radiant Temperature (T_{mrt})

Figure 12 shows a comparison between Tmrt Performance at four points. The data collected from R1, during the daytime, indicated that the reference scenario without any green elements resulted in the highest Tmrt values, reaching a maximum of 83.3 °C at 3:00 p.m. Conversely, mitigation scenarios Sc-A, Sc-B, Sc-C, and Sc-D showed noticeable improvements mainly during the morning hours 7:00 a.m. to 12:00 p.m. and evening hours 4:00 p.m. to 7:00 p.m. Sc-A resulted in an average Tmrt reduction of 8.5 degrees. Sc-B exhibited an average reduction of 15.6 degrees. Similarly, Sc-C, with 50% trees and 50% grass, showed an average reduction of 16 degrees, resembling the performance of Sc-B. However, Sc-D exhibited the most significant improvement, with an average reduction of 17.4 degrees. During nighttime, scenarios involving trees showed a slight increase of 0.6 °C in Tmrt compared to the reference case at 5:00 a.m., while Sc-A demonstrated the best results with an average Tmrt reduction of 1.9 °C. However, an observable increase was noted during specific hours, 1:00 p.m. to 4:00 p.m. in Sc-B, Sc-C, and Sc-D, where trees were present, possibly due to inadequate shading from the trees during these hours. The most pronounced reduction in Tmrt occurred at 5:00 p.m., with Sc-B and Sc-C exhibiting a reduction of 32 degrees and Sc-D recording a reduction of 34 degrees.

The simulated data were collected from R2, and the results indicate no observed improvement in Sc-A compared to the reference case. Sc-B and Sc-C exhibit closely aligned results. The most significant improvements were observed from 7:00 a.m. to 6:00 p.m. The average reduction in Tmrt was 16 degrees, while Sc-D demonstrated an average reduction of 18.7 degrees. In the nighttime period from 7:00 p.m. to 6:00 a.m., Tmrt performance in tree scenarios Sc-B, Sc-C, and Sc-D recorded an increase ranging from 5 to 7 degrees, whereas Sc-A showed no increase in Tmrt performance compared to the reference scenario. Further analysis revealed that the most substantial improvement in thermal performance

occurred during the morning hours from 8:00 a.m. to 10:00 a.m., resulting in a reduction of more than 20 degrees.

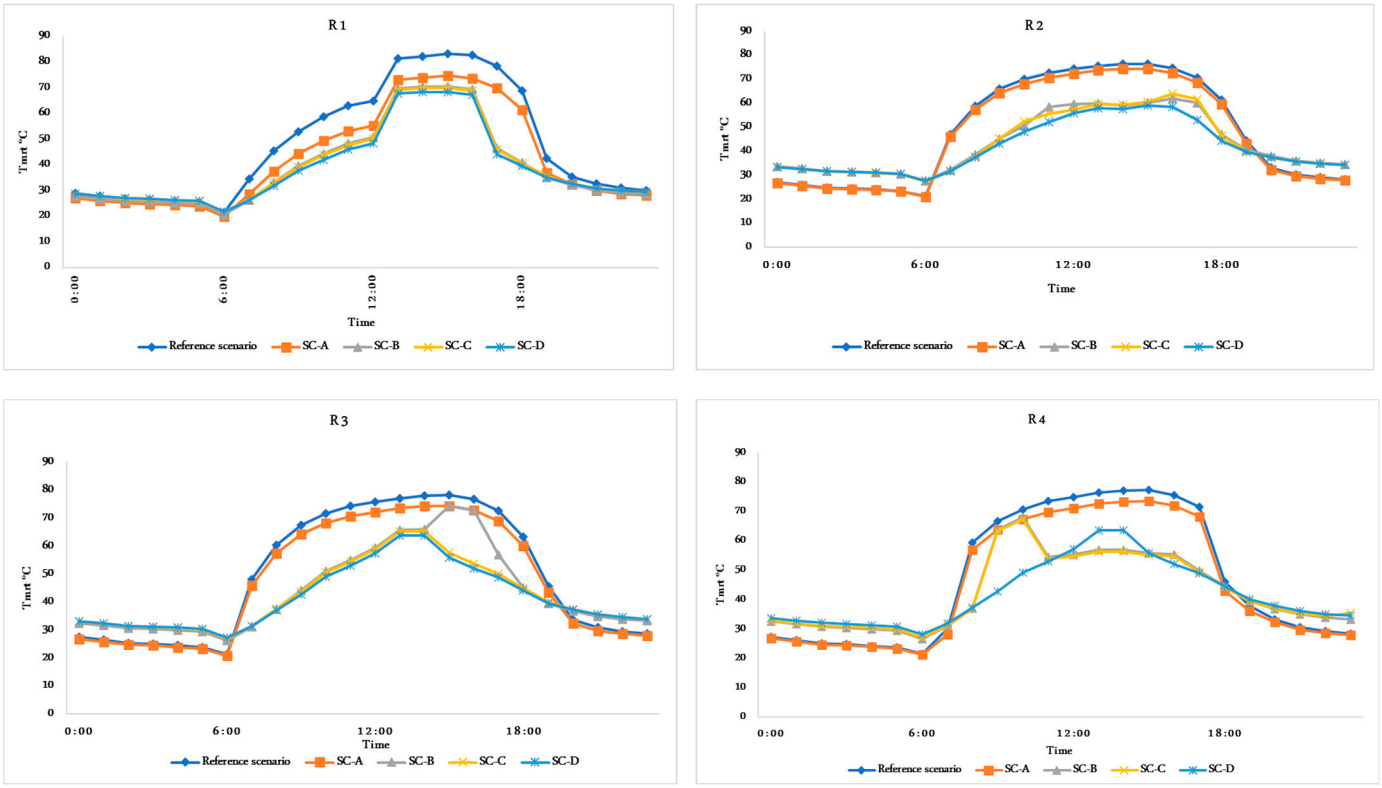

Figure 12. Comparison between T_{mrt} Performance (Mean radiant temperature) at R1, R2, R3, and R4 for Reference scenario and mitigation scenarios A, B, C, and D.

According to the simulated data collected from R3, Sc-A shows only a slight improvement compared to the reference scenario. The average reduction Tmrt during daylight hours from 7:00 a.m. to 6:00 p.m. is 3.4 °C. Sc-B, there is an average Tmrt reduction of 15.4 degrees from 1:00 p.m. to 4:00 p.m., and there is a significant increase of 17 degrees in Tmrt compared to Sc-C and Sc-D. Sc-C and Sc-D showed better results, an average Tmrt reduction of 19 °C and 20 °C degrees from 7:00 a.m. to 7:00 p.m., with minimal reductions observed during the two-hour period from 1:00 p.m. to 2:00 p.m. During the nighttime, Sc-A exhibits the best mitigation of thermal performance, while scenarios involving trees have the opposite effect, increasing Tmrt at night. The most significant improvement in thermal performance is observed at 9:00 a.m. with a reduction ranging from 23 to 24 degrees, followed by 10:00 a.m. with a reduction of 22 degrees.

The simulated data were collected from R4; during daylight hours from 8:00 a.m. to 6:00 p.m., Sc-A exhibits improvement with an average reduction of 3.4 degrees. Sc-B and Sc-C yield closely aligned results, demonstrating notable improvements in Tmrt reduction of 15.5 degrees for Sc-B and 16 for Sc-c. In Sc-D, Tmrt performance shows a more substantial average reduction of 18.2 degrees. However, scenarios Sc-B and Sc-C experience a significant increase during specific two-hour periods, 9:00 a.m. and 10:00 a.m., where Tmrt increases by more than 20 degrees. Sc-D showcases smoother performance throughout all hours. During the nighttime period from 7:00 p.m. to 6:00 a.m., Sc-A in the grass scenario exhibits the best thermal performance at day night hours, with nearly all the reduction observed amounting to 0.5 degrees Celsius compared to the reference scenario. Conversely, tree scenarios result in the opposite effect, increasing Tmrt by 2 to 3 degrees. At 8:00 a.m., the best thermal performance is observed, with a reduction of 22 degrees.

5.4. Evaluating of Physiologically Equivalent Temperature (PET)

The climatic conditions obtained were inputted into the ENVI-met BioMET package to evaluate the thermal performance of the investigated proposed scenarios. This software was utilized to calculate the hourly PET values, which were subsequently employed to assess the appropriate outdoor thermal conditions. Figure 13 shows a comparison between PET performance at four points. The data collected from R1, situated on a pavement tile near a residential building, yielded interesting findings regarding the influence of various scenarios on PET values. During the daytime, the findings indicated that the reference scenario without any green elements resulted in the highest PET values, reaching a maximum of 59.9 °C at 15:00. Conversely, mitigation scenarios Sc-A, Sc-B, Sc-C, and Sc-D showed noticeable improvements, mainly during the morning hours 7:00 to 12:00 and evening hours 16:00 to 19:00. Sc-A, which involved adding 50% grass, resulted in an average PET reduction of 2.5 degrees. Sc-B, combining 25% grass and 25% trees, exhibited an average reduction of 6.4 degrees.

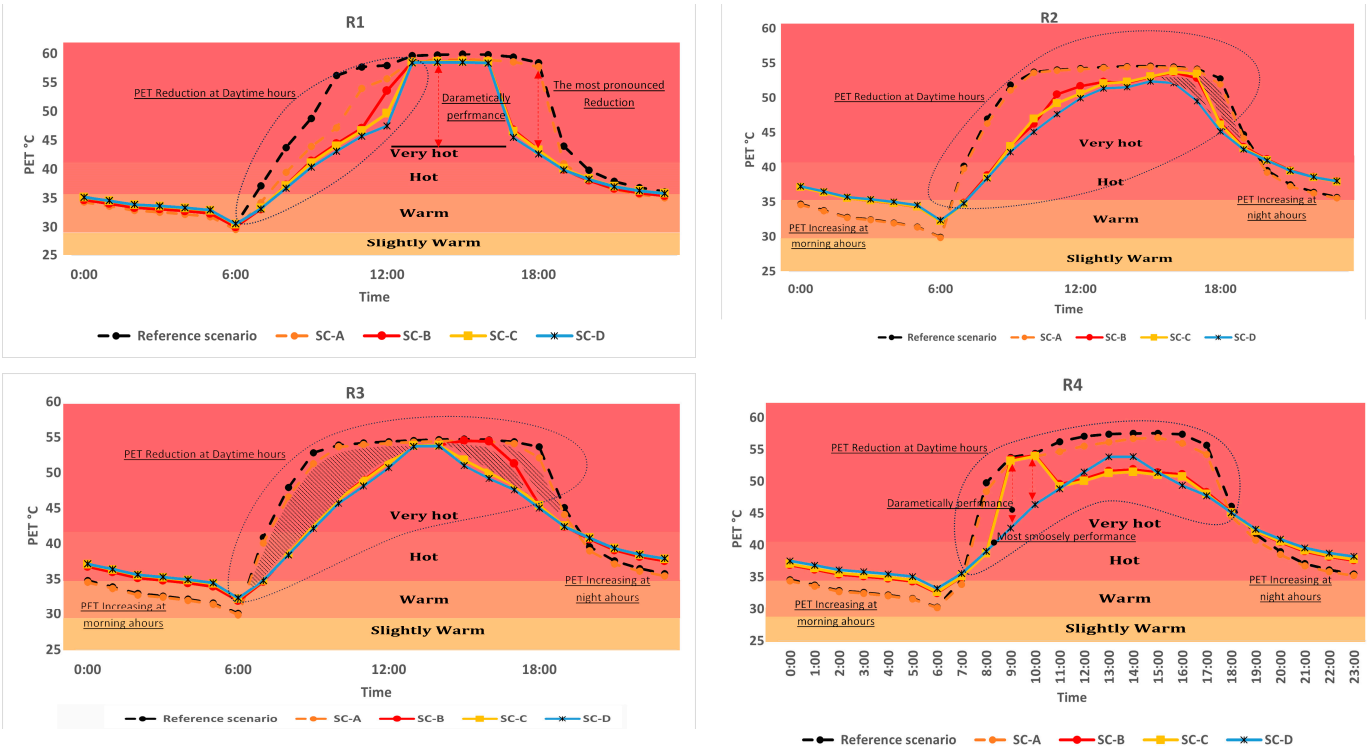

Figure 13. Comparison between PET Performance at R1, R2, R3, and R4 for the Reference case and mitigation scenarios A, B, C, and D. (The dashed polygons delineate periods exhibiting enhanced thermal performance, while shadowed areas represent variations between the investigated scenarios and the reference scenario).

Similarly, Sc-C, with 50% trees and 50% grass, showed an average reduction of 6.8 degrees, resembling the performance of Sc-B. These two scenarios demonstrated minimal differences, indicating similar thermal performance. However, Sc-D, incorporating 75% trees and 50% grass, exhibited the most significant improvement with an average PET reduction of 7.5 degrees. This combination proved most effective in mitigating heat stress and enhancing thermal comfort during daylight hours. During nighttime, scenarios involving trees showed a slight increase of 0.4 °C in PET compared to the reference case, while Sc-A demonstrated the best results with an average PET reduction of 1.2 °C. These findings suggest that including trees during the nighttime did not provide the same level of thermal improvement as grass alone. However, an observable temperature increase was noted during specific hours, 13:00 to 16:00, in Sc-B, Sc-C, and Sc-D, where trees were present, pos-

sibly due to inadequate shading from the trees during these hours. The most pronounced reduction in PET occurred at 6:00, with Sc-B and Sc-C exhibiting a reduction of 14.9 degrees and Sc-D recording a reduction of 15.7 degrees. This highlights the effectiveness of these scenarios in mitigating heat stress and enhancing thermal comfort, particularly during the later hours of the day.

The simulated data were collected from R2, situated on asphalt, and shaded by a leptophylla tree in Sc-B, Sc-C, and Sc-D. The results indicate no observed improvement in Sc-A compared to the reference case. Sc-B and Sc-C exhibit closely aligned results. The most significant improvements were observed from 7:00 to 18:00. During this period, the average reduction in PET was 4.3 degrees, while Sc-D demonstrated an average reduction of 5.5 degrees. In the nighttime period, PET performance in tree scenarios Sc-B, Sc-C, and Sc-D increased from 1.4 to 2.8 degrees, whereas the reference Sc-A showed no increase in PET performance. Further analysis revealed that the most substantial improvement in thermal performance occurred from 8:00 to 10:00, reducing 9.0 degrees.

The simulated data collected from R3, situated on pavement tiles between two residential buildings and shaded by a Nodosa tree in scenarios Sc-B, Sc-C, and Sc-D, reveal the following findings: Sc-A shows only a slight improvement compared to the reference scenario. The average reduction in physiological equivalent temperature (PET) from 7:00 to 18:00 during daylight hours is 0.63 °C. In Sc-B, from 7:00 to 12:00 and from 17:00 to 19:0, there is an average PET reduction of 4.4 degrees; from 13:00 to 16:00, PET significantly increased by 2 to 3 degrees. Sc-c and Sc-D exhibit similar improvements in PET reduction, with Sc-D showing slightly better results. Both scenarios demonstrate an average PET reduction of 5 degrees from 7:00 to 19:00, with minimal reductions of 0.8 °C observed during the two hours from 13:00 to 14:00. During the nighttime, Sc-A exhibits the best mitigation of thermal performance, while scenarios involving trees have the opposite effect, increasing PET at night. The most significant improvement in thermal performance is observed at 8:00, with a reduction of 9 degrees, followed by 10:00, with a reduction of 10 degrees. At 18:00, the reduction is 8 degrees.

The simulated data were collected from R4, situated on grass, and shaded by nodosa trees in scenarios Sc-B, Sc-C, and Sc-D. From 8:00 to 18:00, Sc-A exhibits minimal improvement with an average reduction of 1.1 degrees in PET. Scenarios Sc-B and Sc-C yield closely aligned results, demonstrating notable improvements during daylight hours with an average PET reduction of 5 degrees. In Sc-D, PET performance shows a more substantial average reduction of 6 degrees. However, scenarios Sc-B and Sc-C experience a significant increase in PET during specific two-hour periods, specifically at 9:00 and 10:00, where PET increases by more than 10 degrees. Sc-D showcases smoother performance throughout all hours, likely due to the distribution and increased presence of trees at R4. During the nighttime period from 19:00 to 6:00, Sc-A in the grass scenario exhibits the best thermal performance, with nearly all the reductions observed amounting to a 2 degree Celsius reduction compared to the reference scenario. Conversely, tree scenarios result in the opposite effect, increasing PET by 2 to 3 degrees. At 8:00, the best thermal performance is observed, with a reduction of 10 degrees in PET.

Table 6 presents the thermal distribution map of PET for both the reference and mitigation scenarios. The PET output data were acquired from LEONARDO for the whole district at four different hours: 11:00 a.m., 1:00 p.m., 3:00 p.m., and 5:00 p.m. The results demonstrate a substantial improvement in thermal performance for the vegetation scenarios. However, during the night hour, 5:00 p.m., the PET values tend to increase compared to the Reference scenario; this could be attributed to several factors, such as reduced wind flow and increased RH because of adding trees. Furthermore, the grass scenario shows an increase in PET during daytime hours, which could be attributed to the lower shading effect of grass compared to trees, but a reduction during the night hour (5:00 p.m.), possibly due to the cooling effect of grass through evapotranspiration.

Table 6. Thermal distribution map of PET.

Scenarios	Hours				Key
	11:00 a.m.	1:00 p.m.	3:00 p.m.	5:00 p.m.	
Reference Scenario	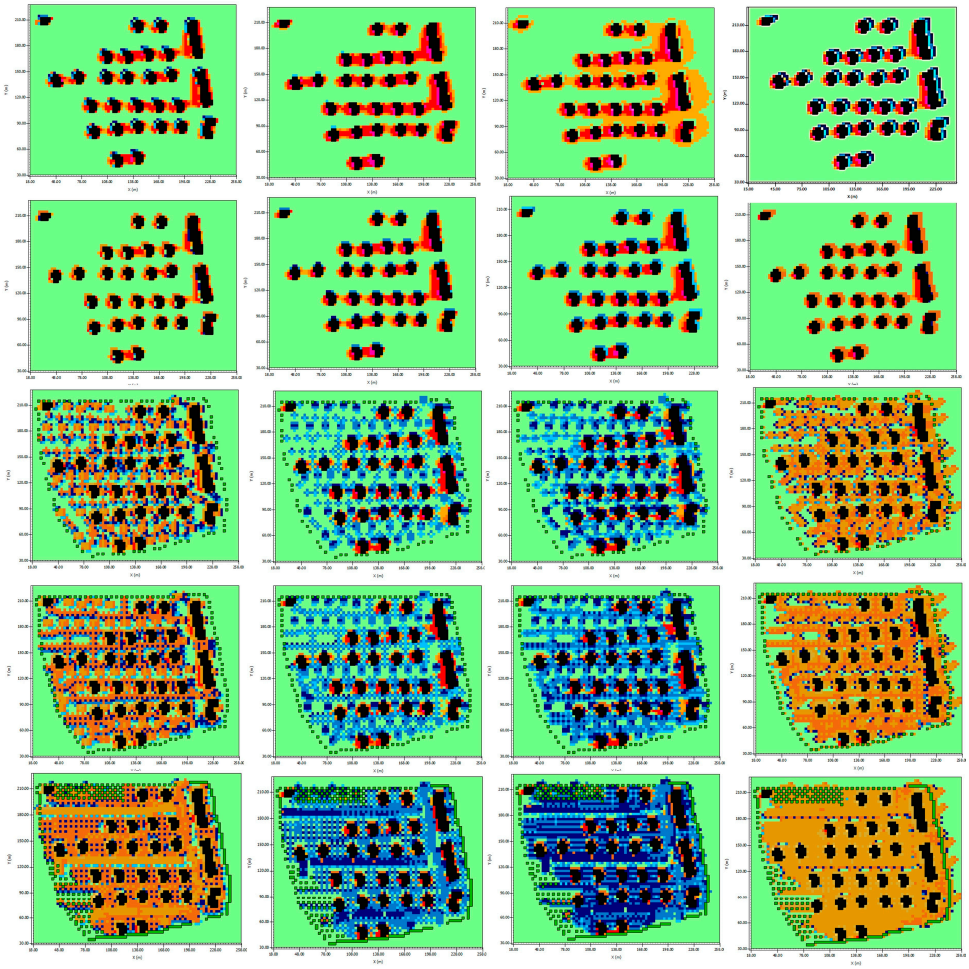				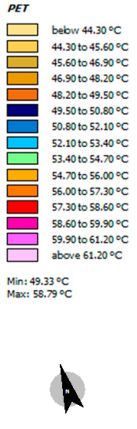
SC-A					
SC-B					
SC-C					
SC-D					

The thermal distribution maps indicated that certain areas, particularly those directly adjacent to building facades, experienced an increase in PET. This could be attributed to the absorption and re-emission of heat by building materials, resulting in localized heat islands. The presence of trees or grass in these areas could help mitigate the heat buildup. The presence of trees or grass in these areas could help mitigate the heat buildup. The maps also revealed that areas facing the direction of the wind exhibited improved PET performance. The wind flow can promote convective cooling, dissipating heat and reducing PET values. This suggests that the strategic placement of trees and grass to align with prevailing wind patterns can enhance overall thermal comfort. Noting that the extent of thermal improvement varies depending on the percentage of trees in the mitigation scenarios, the presence of trees provided effective shading, reducing the overall heat exposure and resulting in lower PET values.

6. Discussion

This study primarily examines the microclimate scale without directly assessing the impact of the investigated trees on the UHI effect in Aswan City. Nonetheless, the findings suggest that strategically planting trees has the potential to mitigate the UHI effect. Apart from providing shading, trees contribute to temperature reduction through processes such

as transpiration and evapotranspiration, which cool the surrounding air and surfaces. To maximize the benefits of each tree species within the urban form, previous studies recommend strategically planting each tree in its most suitable position [36,48]. *Ficus nitida*, with its dense foliage and broad canopy, is advised to be planted in boundary positions. On the other hand, *Cassia leptophylla* and *Cassia nodosa*, with their compact growth habits, are suggested for planting in positions within the urban core.

The simulation results confirm that low-density built-up areas covered by trees experience lower average air temperatures during daytime in the summer compared to unshaded areas, with a reduction of approximately 0.9 K. Outdoor thermal efficiency could be improved gradually by increasing tree cover percentages. These findings align with previous studies reporting a decrease in average ambient air temperature ranging from 0.9 to 2 K in areas with vegetative canopy [48–56]. However, the investigation reveals an inverse thermal performance across all the scenarios during nighttime, consistent with prior research [36,49,52,57]. This phenomenon can be attributed to the characteristics of evergreen trees, which hinder vertical heat transfer and limit heat exchange between the areas below and above the tree canopy during nocturnal hours. As a result, elevated air temperatures (Ta) are observed during the nighttime.

Interestingly, *Ficus nitida* exhibits the least favorable performance among the investigated tree species during nighttime. In hot, arid regions like Aswan, *Ficus nitida* has the potential to contribute to heat-trapping during nighttime due to its ability to retain heat absorbed during the daytime. The dense foliage and thermal properties of *Ficus nitida* create a microclimate that traps heat close to the ground, leading to elevated nighttime temperatures. This effect is particularly prominent in arid environments where moisture in the air is limited, exacerbating the heat-trapping phenomenon associated with *Ficus nitida* [58]. These findings underscore the importance of considering not only the daytime thermal benefits but also the nocturnal thermal behavior of tree species when selecting appropriate vegetation for urban areas.

In terms of Tmrt and PET values, the present study found that all investigated vegetation scenarios contribute to a significant improvement within low-density built-up areas. However, Aboelata and Sodoudi found limited effectiveness of trees in lowering air temperature in low-density urban areas of Cairo [36]. This discrepancy may stem from the higher temperatures and lower humidity levels in Aswan City compared to Cairo, as previously noted in other studies [26,59].

7. Conclusions

This study demonstrates the impact of different vegetation scenarios on thermal comfort and heat stress mitigation within a hot, arid residential urban microclimate. It provides a detailed comparison of different vegetation scenarios (Sc-A, Sc-B, Sc-C, and Sc-D) with a reference scenario regarding their impact on air temperature and thermal performance. For example, Sc-A, which included the addition of 50% grass, resulted in a reduction ranging from 0.02 k to 0.275 k from 8:00 to 19:00. Sc-B, where 25% trees and 50% grass were added, recorded a reduction ranging from 0.12 k to 0.67 k. Sc-C, which included 50% trees, reduced from 0.13 k to 0.78 k. Lastly, Sc-D with 75% trees exhibited the best reduction, ranging from 0.2 k to 0.92 k.

Moreover, the results show that scenarios with a higher percentage of trees exhibited the best PET reduction, indicating effective heat stress mitigation and thermal comfort enhancement during daylight hours. The most significant reduction in PET, with a decrease of 15.7 degrees, was observed in the afternoon. Additionally, PET reductions of up to 10 °C were recorded during the morning hours compared to the non-vegetated base case. Trees exhibited a stronger cooling effect than grass, with the 75/50 tree/grass scenario lowering PET by an average of 7.5 °C during daylight hours, while the 50% grass scenario resulted in a reduction of only 2.5 °C. The strategic placement of trees and grass aligned with prevailing wind patterns can enhance overall thermal comfort.

However, including trees during nighttime did not provide the same level of thermal improvement as grasses alone. Based on the analysis's findings, it is evident that the greening scenarios had varying effects on thermal performance during both daytime and nighttime. Including trees during the nighttime did not provide the same level of thermal improvement as grasses alone, with an observable temperature increase noted during specific hours. However, during the daytime, scenarios involving trees showed noticeable improvements, particularly during specific hours.

Spatial analysis reveals localized variations, with peripheral areas exhibiting greater mitigation than central zones shielded from breezes. This highlights the need for optimized vegetation planning tailored to neighborhood layouts. Although air temperature reductions were more modest ($\leq$1 °C), the study confirms urban greenery's passive cooling potential.

The results highlight urban greenery's potential to minimize heat stress passively but suggest the need for careful vegetative planning tailored to local climate and morphology. Further work optimizing species selection, density, configuration, and interactions with the built environment can help translate these improvements into effective, site-specific design guidance for enhancing resilient outdoor thermal comfort.

Author Contributions: Conceptualization, A.E.L.M. and A.R.; methodology, J.N.; software, A.R. and J.N.; validation, A.E.L.M., M.M.G. and A.R.; formal analysis, A.R.; investigation, J.N. and A.R.; resources, M.M.G.; data curation, J.N.; writing—original draft preparation, J.N. and A.R.; writing—review and editing M.M.G.; visualization, J.N. and A.R.; project administration, M.M.G.; funding acquisition, M.M.G. All authors have read and agreed to the published version of the manuscript.

Funding: This research was funded by the Vice President for Graduate Studies, Research and Business (GRB) at Dar Al-Hekma University, Jeddah, under grant no. (RFC/23-24/03). The author, therefore, acknowledges with thanks GRB for technical and financial support.

Institutional Review Board Statement: Not applicable.

Informed Consent Statement: Not applicable.

Data Availability Statement: Data are contained within the article.

Conflicts of Interest: The authors declare no conflicts of interest.

References

1. Roshan, G.R.; Ranjbar, F.; Orosa, J.A. Simulation of global warming effect on outdoor thermal comfort conditions. *Int. J. Environ. Sci. Technol.* **2010**, *7*, 571–580. [CrossRef]
2. Mahmoud, A.R.A.; Aly, A.M.; Hassan, M.H. Evaluating the thermal performance of urban spaces in aswan city "a case study of saad zaghloul street. *J. Eng. Sci.* **2015**, *43*, 766–782. [CrossRef]
3. Kim, Y.; An, S.M.; Eum, J.-H.; Woo, J.-H. Analysis of thermal environment over a small-scale landscape in a densely built-up Asian megacity. *Sustainability* **2016**, *8*, 358. [CrossRef]
4. Gomaa, M.; Ragab, A. Investigating the Spatial Autocorrelation of Surface-Air Temperature for Different Ground Materials in Hot Desert Climate. *Egypt. Int. J. Eng. Sci. Technol.* **2022**, *39*, 49–59. [CrossRef]
5. Taleghani, M.; Sailor, D.; Ban-Weiss, G.A. Micrometeorological simulations to predict the impacts of heat mitigation strategies on pedestrian thermal comfort in a Los Angeles neighborhood. *Environ. Res. Lett.* **2016**, *11*, 024003. [CrossRef]
6. Patel, S.; Indraganti, M.; Jawarneh, R.N. A comprehensive systematic review: Impact of Land Use/Land Cover (LULC) on Land Surface Temperatures (LST) and outdoor thermal comfort. *Build. Environ.* **2023**, *249*, 111130. [CrossRef]
7. Sharifi, A. Co-benefits and synergies between urban climate change mitigation and adaptation measures: A literature review. *Sci. Total Environ.* **2021**, *750*, 141642. [CrossRef] [PubMed]
8. McEvoy, D.; Lindley, S.; Handley, J. Adaptation and mitigation in urban areas: Synergies and conflicts. *Proc. Inst. Civ. Eng. Munic. Eng.* **2006**, *159*, 185–191. [CrossRef]
9. Mahmoud, H.; Ragab, A. Urban geometry optimization to mitigate climate change: Towards energy-efficient buildings. *Sustainability* **2020**, *13*, 27. [CrossRef]
10. Abdelhafez, M.H.H.; Altaf, F.; Alshenaifi, M.; Hamdy, O.; Ragab, A. Achieving effective thermal performance of street canyons in various climatic zones. *Sustainability* **2022**, *14*, 10780. [CrossRef]
11. Abdallah, A.S.H. Passive design strategies to improve student thermal comfort in Assiut University: A field study in the Faculty of Physical Education in hot season. *Sustain. Cities Soc.* **2022**, *86*, 104110. [CrossRef]
12. Mahmoud, R.M.A.; Abdallah, A.S.H. Assessment of outdoor shading strategies to improve outdoor thermal comfort in school courtyards in hot and arid climates. *Sustain. Cities Soc.* **2022**, *86*, 104147. [CrossRef]

13. Stocco, S.; Cantón, M.A.; Correa, E. Evaluation of design schemes for urban squares in arid climate cities, Mendoza, Argentina. In *Building Simulation*; Springer: Berlin/Heidelberg, Germany, 2021; Volume 14, pp. 763–777.
14. Rodríguez-Algeciras, J.; Tablada, A.; Nouri, A.S.; Matzarakis, A. Assessing the influence of street configurations on human thermal conditions in open balconies in the Mediterranean climate. *Urban Clim.* **2021**, *40*, 100975. [CrossRef]
15. Okumus, D.E.; Terzi, F. Evaluating the role of urban fabric on surface urban heat island: The case of Istanbul. *Sustain. Cities Soc.* **2021**, *73*, 103128. [CrossRef]
16. Taleghani, M.; Kleerekoper, L.; Tenpierik, M.; Van Den Dobbelsteen, A. Outdoor thermal comfort within five different urban forms in the Netherlands. *Build. Environ.* **2015**, *83*, 65–78. [CrossRef]
17. Mahmoud, H.; Ragab, A. Impact of urban geometry on cooling loads in Egypt: Case study: A social residential compound in New Aswan city. In Proceedings of the 2020 9th International Conference on Power Science and Engineering (ICPSE), London, UK, 23–25 October 2020; IEEE: Piscataway, NJ, USA; pp. 71–75.
18. *ISO 7730:2005*; Ergonomics of the Thermal Environment—Analytical Determination and Interpretation of Thermal Comfort Using Calculation of the PMV and PPD Indices and Local Thermal Comfort Criteria. ISO: Geneva, Switzerland, 1984.
19. Ribeiro, K.F.A.; Justi, A.C.A.; Novais, J.W.Z.; de Moura Santos, F.M.; Nogueira, M.C.d.J.A.; Miranda, S.A.; Marques, J.B. Calibration of the Physiological Equivalent Temperature (PET) index range for outside spaces in a tropical climate city. *Urban Clim.* **2022**, *44*, 101196. [CrossRef]
20. Chen, L.; Ng, E. Simulation of the effect of downtown greenery on thermal comfort in subtropical climate using PET index: A case study in Hong Kong. *Archit. Sci. Rev.* **2013**, *56*, 297–305. [CrossRef]
21. Walther, E.; Goestchel, Q. The PET comfort index: Questioning the model. *Build. Environ.* **2018**, *137*, 1–10. [CrossRef]
22. Höppe, P. The physiological equivalent temperature–a universal index for the biometeorological assessment of the thermal environment. *Int. J. Biometeorol.* **1999**, *43*, 71–75. [CrossRef]
23. Brosy, C.; Zaninovic, K.; Matzarakis, A. Quantification of climate tourism potential of Croatia based on measured data and regional modeling. *Int. J. Biometeorol.* **2014**, *58*, 1369–1381. [CrossRef]
24. Deb, C.; Ramachandraiah, A. The significance of physiological equivalent temperature (PET) in outdoor thermal comfort studies. *Int. J. Eng. Sci. Technol.* **2010**, *2*, 2825–2828.
25. Lau, K.K.-L.; Chung, S.C.; Ren, C. Outdoor thermal comfort in different urban settings of sub-tropical high-density cities: An approach of adopting local climate zone (LCZ) classification. *Build. Environ.* **2019**, *154*, 227–238. [CrossRef]
26. Ragab, A.; Abdelrady, A. Impact of green roofs on energy demand for cooling in Egyptian buildings. *Sustainability* **2020**, *12*, 5729. [CrossRef]
27. Akbari, H.; Matthews, H.D. Global cooling updates: Reflective roofs and pavements. *Energy Build.* **2012**, *55*, 2–6. [CrossRef]
28. Rosenfeld, A.H.; Akbari, H.; Bretz, S.; Fishman, B.L.; Kurn, D.M.; Sailor, D.; Taha, H. Mitigation of urban heat islands: Materials, utility programs, updates. *Energy Build.* **1995**, *22*, 255–265. [CrossRef]
29. Onyango, S.A.; Mukundi, J.B.; Ochieng'Adimo, A.; Wesonga, J.M.; Sodoudi, S. Variability of In-Situ Plant Species Effects on Microclimatic Modification in Urban Open Spaces of Nairobi, Kenya. *Curr. Urban Stud.* **2021**, *9*, 126. [CrossRef]
30. Bruse, M. Modelling and strategies for improved urban climates. In Proceedings of the International Conference on Urban Climatology & International Congress of Biometeorology, Sydney, Australia, 8–12 November 1999; Citeseer: Gaithersburg, MD, USA, 1999; pp. 8–12.
31. Erell, E.; Zhou, B. The effect of increasing surface cover vegetation on urban microclimate and energy demand for building heating and cooling. *Build. Environ.* **2022**, *213*, 108867. [CrossRef]
32. Zhao, J.; Zhao, X.; Liang, S.; Zhou, T.; Du, X.; Xu, P.; Wu, D. Assessing the thermal contributions of urban land cover types. *Landsc. Urban Plan.* **2020**, *204*, 103927. [CrossRef]
33. Chapman, S.; Thatcher, M.; Salazar, A.; Watson, J.E.; McAlpine, C.A. The effect of urban density and vegetation cover on the heat island of a subtropical city. *J. Appl. Meteorol. Climatol.* **2018**, *57*, 2531–2550. [CrossRef]
34. Jim, C.Y. Effect of vegetation biomass structure on thermal performance of tropical green roof. *Landsc. Ecol. Eng.* **2012**, *8*, 173–187. [CrossRef]
35. Weng, Q.; Liu, H.; Lu, D. Assessing the effects of land use and land cover patterns on thermal conditions using landscape metrics in city of Indianapolis, United States. *Urban Ecosyst.* **2007**, *10*, 203–219. [CrossRef]
36. Aboelata, A.; Sodoudi, S. Evaluating the effect of trees on UHI mitigation and reduction of energy usage in different built up areas in Cairo. *Build. Environ.* **2020**, *168*, 106490. [CrossRef]
37. Srivanit, M.; Hokao, K. Evaluating the cooling effects of greening for improving the outdoor thermal environment at an institutional campus in the summer. *Build. Environ.* **2013**, *66*, 158–172. [CrossRef]
38. Rose, A.L. Impact of urbanization on the thermal comfort conditions in the hot humid city of Chennai, India. In Proceedings of the Recent Advances in Space Technology Services and Climate Change 2010 (RSTS & CC-2010), Chennai, India, 13–15 November 2010; pp. 262–267.
39. Amirtham, L.R.; Horrison, E.; Rajkumar, S. Study on the microclimatic conditions and thermal comfort in an institutional campus in hot humid climate. In Proceedings of the 30th International PLEA Conference, Ahmedabad, India, 16–18 December 2014; pp. 16–18.
40. Fahmy, M.; Sharples, S. On the development of an urban passive thermal comfort system in Cairo, Egypt. *Build. Environ.* **2009**, *44*, 1907–1916. [CrossRef]

41. Dohsi, K.; Djaghrouri, D.; Benabbas, M. Effect of vegetation on outdoor thermal comfort in hot arid regions, a lesson of sustainability from the traditional Ksar of Ain Madhi, Algeria. *Technium Soc. Sci. J.* **2022**, *38*, 794. [CrossRef]
42. Louafi, S.; Abdou, S.; Reiter, S. Effect of vegetation cover on thermal and visual comfort of pedestrians in urban spaces in hot and dry climate. *Nat. Technol.* **2017**, *17*, 30B.
43. Roberto, B.; Barkmeijer, J.; Palmer, T.N.; David, R. *Current Status and Future Developments of the ECMWF Ensemble Prediction System*; ECMWF: Reading, UK, 1999.
44. Onset Computer Corporation. HOBO MX1104 Data Logger Specifications. 2024. Available online: https://www.onsetcomp.com/contact/support (accessed on 14 April 2024).
45. Elnabawi, M.H.; Hamza, N.; Raveendran, R. 'Super cool roofs': Mitigating the UHI effect and enhancing urban thermal comfort with high albedo-coated roofs. *Results Eng.* **2023**, *19*, 101269. [CrossRef]
46. Kim, J.; Hong, T.; Koo, C.-W. Economic and environmental evaluation model for selecting the optimum design of green roof systems in elementary schools. *Environ. Sci. Technol.* **2012**, *46*, 8475–8483. [CrossRef] [PubMed]
47. Fahmy, M.; El-Hady, H.; Mahdy, M.; Abdelalim, M.F. On the green adaptation of urban developments in Egypt; predicting community future energy efficiency using coupled outdoor-indoor simulations. *Energy Build.* **2017**, *153*, 241–261. [CrossRef]
48. Tan, Z.; Lau, K.K.-L.; Ng, E. Planning strategies for roadside tree planting and outdoor comfort enhancement in subtropical high-density urban areas. *Build. Environ.* **2017**, *120*, 93–109. [CrossRef]
49. Park, M.; Hagishima, A.; Tanimoto, J.; Narita, K.-i. Effect of urban vegetation on outdoor thermal environment: Field measurement at a scale model site. *Build. Environ.* **2012**, *56*, 38–46. [CrossRef]
50. Wang, Y.; Bakker, F.; de Groot, R.; Wortche, H.; Leemans, R. Effects of urban trees on local outdoor microclimate: Synthesizing field measurements by numerical modelling. *Urban Ecosyst.* **2015**, *18*, 1305–1331. [CrossRef]
51. Doick, K.J.; Peace, A.; Hutchings, T.R. The role of one large greenspace in mitigating London's nocturnal urban heat island. *Sci. Total Environ.* **2014**, *493*, 662–671. [CrossRef] [PubMed]
52. Akbari, H. Shade trees reduce building energy use and CO_2 emissions from power plants. *Environ. Pollut.* **2002**, *116*, S119–S126. [CrossRef] [PubMed]
53. Takebayashi, H.; Moriyama, M. Study on the urban heat island mitigation effect achieved by converting to grass-covered parking. *Sol. Energy* **2009**, *83*, 1211–1223. [CrossRef]
54. Ghaffarianhoseini, A.; Berardi, U.; Ghaffarianhoseini, A. Thermal performance characteristics of unshaded courtyards in hot and humid climates. *Build. Environ.* **2015**, *87*, 154–168. [CrossRef]
55. Mahmoud, H.; Ragab, A. Thermal Performance Evaluation of Unshaded Courtyards in Egyptian Arid Regions. *Smart Sustain. Plan. Cities Reg. Results SSPCR* **2021**, *3*, 109–121.
56. Bowler, D.E.; Buyung-Ali, L.; Knight, T.M.; Pullin, A.S. Urban greening to cool towns and cities: A systematic review of the empirical evidence. *Landsc. Urban Plan.* **2010**, *97*, 147–155. [CrossRef]
57. Heisler, G.M.; Grant, R.H. Ultraviolet radiation in urban ecosystems with consideration of effects on human health. *Urban Ecosyst.* **2000**, *4*, 193–229. [CrossRef]
58. Freer-Smith, P.; El-Khatib, A.; Taylor, G. Capture of particulate pollution by trees: A comparison of species typical of semi-arid areas (Ficus nitida and Eucalyptus globulus) with European and North American species. *Water Air Soil Pollut.* **2004**, *155*, 173–187. [CrossRef]
59. Mahdy, M.; Nikolopoulou, M.; Fahmy, M. Climate change scenarios effects on residential buildings shading strategies in Egypt. In Proceedings of the Building Simulation—Towards Sustainable Green Built Environment, Cairo, Egypt, 23–24 June 2013.